

## Elementary ${}^2\text{H}(p,p'\pi^+)n$ reaction

Bijoy Kundu, B. K. Jain, and A. B. Santra

*Nuclear Physics Division, Bhabha Atomic Research Centre, Mumbai-400 085, India*

(Received 2 February 1998)

A detailed study of the elementary  ${}^2\text{H}(p,p'\pi^+)n$  reaction is presented using the  $\Delta$  isobar model. In this model, in the first step one of the two protons in the initial state gets excited to  $\Delta$ . This, in the second step, decays into a nucleon and a pion. For the  $pp \rightarrow N\Delta$  step the parametrized form of the distorted-wave Born approximation  $t$  matrix of Jain and Santra, which reproduces most of the available data on  $pp \rightarrow n\Delta^{++}$ , is used. The cross sections studied include the outgoing proton momentum spectra in coincidence with the pion, the outgoing pion momentum spectra, and the integrated total cross section. We find that all the calculated numbers are in good agreement with the corresponding measured cross sections. [S0556-2813(98)01609-4]

PACS number(s): 25.40.Ve, 13.75.-n, 25.55.-e

### I. INTRODUCTION

In the past various authors [1,2], including two of the present authors (Jain and Santra), have analyzed theoretically the data on the  $pp \rightarrow n\Delta^{++}$  reaction to extract the potential for  $pp \rightarrow N\Delta$  transition. In them, the calculations of Jain *et al.* [2] were done in the distorted-wave Born approximation (DWBA) and those of Dmitriev [1] were done in the plane-wave Born approximation (PWBA). They concluded that the spin averaged data on the  $pp \rightarrow N\Delta$  reaction can be reproduced very well by a one pion-exchange potential with the length parameter  $\Lambda_\pi$  around 1–1.2 GeV/ $c$  in DWBA and around 650 MeV/ $c$  in the PWBA. The difference in the two values of  $\Lambda_\pi$  is due to distortion effects. In fact, subsequently, when Jain *et al.* parametrized their DWBA  $t$  matrix [3], they found that the imaginary part of this  $t$  matrix is very weak and the real part resembles to a great extent the one pion-exchange potential, with  $\Lambda_\pi$  reduced to around 650 MeV/ $c$ .

The experimental data which the above studies used were somewhat inclusive [4,5]. They were deduced from the  $pp \rightarrow np'\pi^+$  reaction data which did not have the complete exclusive kinematics. The  $\Delta$  was identified in them by seeing a bump in the missing mass spectrum. A kinematically complete data set, however, exists on the  $pp \rightarrow p'\pi^+n$  reaction at 800 MeV beam energy from LAMPF due to Hancock *et al.* [6]. They are a good coincidence data, and, thus, provide an excellent opportunity to test in detail the correctness of the  $pp \rightarrow n\Delta^{++}$  DWBA  $t$  matrix developed by two of us earlier [3]. In the present paper we analyze the LAMPF data using this  $t$  matrix. This includes the analysis of the various proton and pion energy spectra measured in coincidence and the total integrated cross section for the  $pp \rightarrow p'\pi^+n$  reaction. We assume that the  $pp \rightarrow p'\pi^+n$  reaction proceeds in two steps. In the first step, one of the protons in the entrance channel gets converted to  $\Delta$ , and in the second step this  $\Delta$  decays into a pion and a nucleon. The transition matrix for the  $pp \rightarrow \Delta N$  step is taken to be the DWBA  $t$  matrix mentioned above. The decay of the  $\Delta$  is described by the pseudovector nonrelativistic Lagrangian,

$$L_{\pi N\Delta} = i \frac{f_\pi^*}{m_\pi} (\mathbf{S} \cdot \boldsymbol{\kappa}_\pi) (\mathbf{T} \cdot \boldsymbol{\phi}), \quad (1)$$

where  $f_\pi^*$  is the coupling constant at the  $\pi N\Delta$  vertex.  $\mathbf{S}$  and  $\mathbf{T}$  are the spin and isospin transition operators, respectively. This framework for the  $pp \rightarrow p\pi^+n$  reaction includes in a certain way the final state interaction (FSI) amongst  $p\pi^+n$  in the final state. The FSI consists of the interaction between  $p$  and  $\pi^+$  and between the  $p\pi^+$  pair and the recoiling neutron. The dominant effect of the interaction between  $p$  and  $\pi^+$  is to produce the  $\Delta^{++}$  resonance. This is explicitly included in our framework. The interaction between  $p\pi^+$  and the neutron in our framework is approximated by that between the  $\Delta^{++}$  and the neutron. A recent work by Jain and Kundu [7] on the  $\Delta$  decay in nuclear medium suggests that this approximation is reasonably good.

The  $pp \rightarrow np'\pi^+$  process has also been worked out in the literature by Engel *et al.* [8]. However, these calculations use plane waves for the continuum particles. Thus, unlike our work, this work does not include the effect of distortions in the entrance and the exit channels.

Inclusion or omission of  $\rho$  exchange in the description of the  $pp \rightarrow n\Delta^{++}$  reaction has been the topic of much debate in the literature. The general conclusion is that the spin averaged data on the  $pp \rightarrow \Delta^{++}n$  reaction are well reproduced by one pion-exchange potential only [1,2,9,10]. Any attempt to include the  $\rho$  exchange worsens the agreement with the experiments, and yield unsatisfactory results. In this context it is also interesting to see the work of Jain *et al.* [11] which discusses the relative importance of  $\rho$  exchange in  $p(n,p)n$  and  $p(p,n)\Delta^{++}$  reactions. They conclude that, while it is absolutely essential to include the  $\rho$  exchange in the description of the  $p(n,p)n$  reaction, the  $\rho$  exchange is not required for accounting the  $p(p,n)\Delta^{++}$  data. This study deals with the spin averaged cross sections. A recent theoretical study on the microscopic structure of the  $\rho N\Delta$  vertex by Haider *et al.* [12] supports this conclusion. They find that the microscopically calculated value of the  $f_{\rho N\Delta}$  coupling constant is much smaller than what is normally assumed. The measured spin averaged cross sections on nuclei in charge exchange reactions are also reproduced with only a pion exchange [13]. It is, however, true that the measurements of Prout *et al.* [14] with a polarized proton beam on nuclei, and earlier by Ellegaard *et al.* [15] do show a large transverse part. But, as shown by Dmitriev [13] and Sams *et al.* [16], large

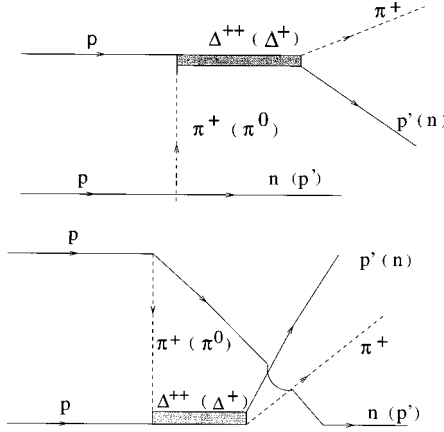


FIG. 1. The direct and exchange diagrams for the  $\Delta$  excitation.

transverse contribution can also arise from the distortion of the continuum particles. All these discussions thus suggest that, at best, the role of  $\rho$  exchange in the charge-exchange reaction in the  $\Delta$  region is controversial. The spin averaged cross sections do not need it, the spin transfer measurements show some indications for it. Since the present work deals with the spin averaged cross sections, our use of one pion exchange is consistent with other work in this field.

In Sec. II we write the formalism for the  $pp \rightarrow np' \pi^+$  process. Section III gives calculated cross sections for the proton and pion energy spectra at 800 MeV beam energy and the total cross section from 500 MeV to 2 GeV. These results are compared with the available experimental cross sections. Good agreement is obtained.

## II. FORMALISM

The cross section for the  $pp \rightarrow np' \pi^+$  process is given by

$$d\sigma = \langle |t_{pp \rightarrow p' \pi^+ n}|^2 \rangle [\text{PS}], \quad (2)$$

where the angular brackets denote the sum and average over the spins in the initial and final states, respectively. [PS] is the factor associated with the phase space and the beam current. For the proton and pion detected in coincidence in the final state, in the lab frame it is given by

$$[\text{PS}] = \frac{m_p^2 m_n k_p'^2 k_\pi^3}{2(2\pi)^5 k_p E_p' k_\pi^2 (E_i - E_p') - E_\pi |(\mathbf{k}_p - \mathbf{k}_p') \cdot \mathbf{k}_\pi|} \times d\Omega_p' d\Omega_\pi dk_p'. \quad (3)$$

$t_{pp \rightarrow p' \pi^+ n}$  is the  $t$  matrix for the  $pp \rightarrow p' \pi^+ n$  process. It consists of two parts: one corresponding to the excitation of the proton in the initial state to  $\Delta^{++}$  and another corresponding to its excitation to  $\Delta^+$  (Fig. 1). That is,

$$t_{pp \rightarrow p' \pi^+ n} = t^{\Delta^{++}} + t^{\Delta^+}. \quad (4)$$

Furthermore, because of the antisymmetrization of the protons, each  $t$  matrix in turn consists of two terms, one corresponding to the excitation of the beam proton and another corresponding to the excitation of the target proton. We call them ‘‘direct’’ and ‘‘exchange’’ terms, respectively.

Putting everything together, we get

$$t_{pp \rightarrow NN\pi} = \sum_{\Delta} \langle N\pi | \mathbf{S} \cdot \boldsymbol{\kappa}_\pi \mathbf{T} \cdot \boldsymbol{\phi}_\pi | \Delta \rangle G_{\Delta} \langle t_{pp \rightarrow N\Delta} \rangle, \quad (5)$$

where  $N$  represents a proton or a neutron in the final state corresponding to the decay of  $\Delta^{++} \rightarrow \pi^+ p$  and  $\Delta^+ \rightarrow \pi^+ n$ , respectively.  $\Delta$  stands for a  $\Delta^{++}$  or  $\Delta^+$  excitation in the intermediate state.  $\boldsymbol{\kappa}_\pi$  at the  $\Delta$ -decay vertex is the outgoing pion momentum in the  $\pi N$  center-of-mass. It is given by

$$\boldsymbol{\kappa}_\pi(\mu^2, m_\pi^2) = [(\mu^2 + m^2 - m_\pi^2)^2 / 4\mu^2 - m^2]^{1/2}. \quad (6)$$

This relation reflects the restrictions on the available phase space for the decay of a  $\Delta$  of mass  $\mu$  into an on-shell pion of mass  $m_\pi$  ( $=140$  MeV) and a nucleon. Since the final outgoing pion is on shell, the  $\Delta N \pi$  vertex does not contain the usual form factor  $F^*$ .  $G_{\Delta}$  in Eq. (5) is the delta propagator. Its form is taken as

$$G_{\Delta} = \frac{2m_{\Delta}}{\mu^2 - m_{\Delta}^2 + i\Gamma_{\Delta}m_{\Delta}}, \quad (7)$$

where  $m_{\Delta}$  ( $=1232$  MeV) and  $\Gamma_{\Delta}$  are the resonance parameters associated with a free  $\Delta$ . The free width  $\Gamma_{\Delta}$  depends upon the invariant mass and is written as

$$\Gamma_{\Delta} = \Gamma_0 \left[ \frac{k(\mu^2, m_\pi^2)}{k(m_{\Delta}^2, m_\pi^2)} \right]^3 \frac{k^2(m_{\Delta}^2, m_\pi^2) + \gamma^2}{k^2(\mu^2, m_\pi^2) + \gamma^2}, \quad (8)$$

with  $\Gamma_0 = 120$  MeV and  $\gamma = 200$  MeV.  $\mu$  is the invariant mass of the  $N\pi^+$  system and is given by

$$\mu^2 = (E_N + E_\pi)^2 - (\mathbf{k}_N + \mathbf{k}_\pi)^2. \quad (9)$$

$t_{pp \rightarrow N\Delta}$  is the DWBA  $t$  matrix for the  $pp \rightarrow N\Delta$  transition. Following Jain and Santra [2], it is given by

$$t_{pp \rightarrow N\Delta} = (\chi_{\mathbf{k}_f}^-, \langle n\Delta^{++} | v_\pi | \{pp\} \rangle, \chi_{\mathbf{k}_i}^+), \quad (10)$$

where curly brackets around  $pp$  represent the antisymmetrization of the  $pp$  wave function.  $v_\pi$  is the one pion-exchange potential for  $pp \rightarrow N\Delta$  transition.  $\chi$ 's are the distorted waves. They describe the elastic scattering of the  $pp$  and the  $n\Delta$  systems. Jain and Santra [4] have evaluated Eq. (10) using eikonal approximation for  $\chi$ 's. With  $\Lambda_\pi = 1$  GeV/ $c$  at both the  $\pi NN$  and  $\pi N\Delta$  vertices, they found that this  $t$  matrix reproduces the available experimental data on this reaction over a large energy range very well.

Jain and Santra also found that their DWBA  $t$  matrix can be easily parametrized [3]. The parametrized  $t$  matrix is complex, but its imaginary part is very weak. The real part resembles very much with the one pion-exchange potential with its length parameter  $\Lambda_\pi$ , reduced to around 600–700 MeV/ $c$ . For the present calculations, instead of repeating the full calculation of the  $t$  matrix, we have used the parametrized form, i.e.,

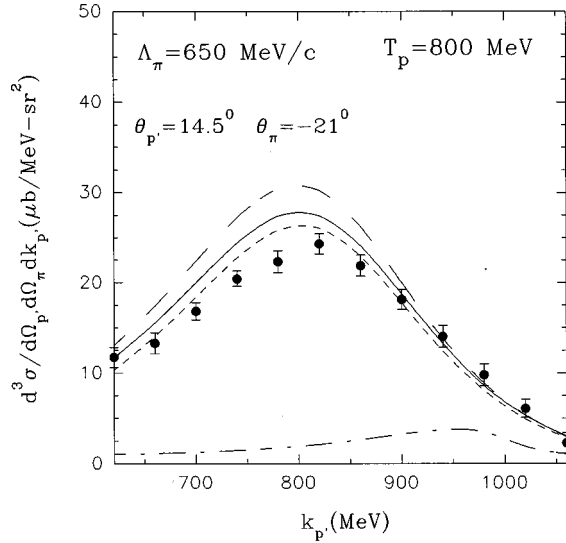


FIG. 2. The outgoing proton momentum spectrum in coincidence with the pion.  $T_p = 800$  MeV.  $\theta'_p = 14.5^\circ$ , and  $\theta_\pi = -21^\circ$ . The experimental points are from Ref. [6]. The long-dashed curve is calculated using the direct  $\Delta^{++}$  diagram and the short-dashed curve includes both the direct and the exchange  $\Delta^{++}$  diagrams. The solid curve is calculated using both the  $\Delta^{++}$  and  $\Delta^+$  diagrams added coherently. The dash-dot curve is the  $\Delta^+$  contribution multiplied by 5.  $\Lambda_\pi = 650$  MeV/c.

$$t_{pp \rightarrow N\Delta} \approx v_{\pi}^{pp \rightarrow N\Delta} (\Lambda_\pi = 650 \text{ MeV}/c)$$

$$= -\frac{ff^*}{m_\pi^2} FF^* \frac{\mathbf{S}^+ \cdot \mathbf{q} \sigma \cdot \mathbf{q}}{m_\pi^2 + q^2 - \omega^2} \mathbf{T}^+ \cdot \boldsymbol{\tau}, \quad (11)$$

where  $f$  and  $f^*$  at the  $\pi NN$  and  $\pi N\Delta$  vertices are 1.008 and 2.156, respectively [17].  $\mathbf{q}$  is the momentum transfer in the pion-nucleon rest frame. Since the exchanged pion is virtual, it is not straightforward to define this momentum quite unambiguously. For the  $\pi N\Delta$  vertex we use the following Galilean invariant form:

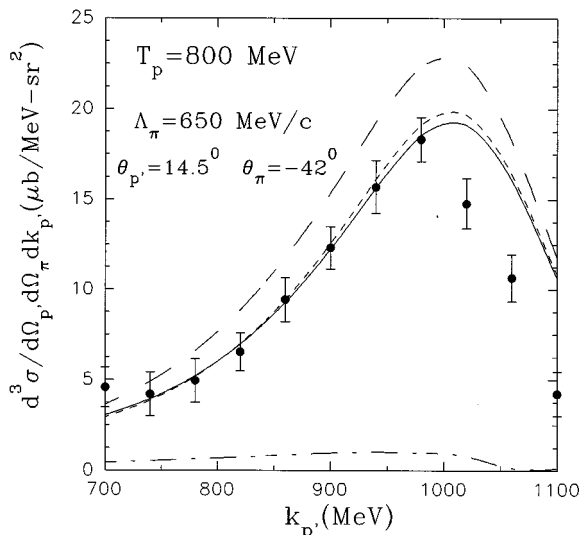


FIG. 3. Same as Fig. 2 with  $\theta'_p = 14.5^\circ$  and  $\theta_\pi = -42^\circ$ . Experimental points are from Ref. [6]. All the curves have the same meaning as in Fig. 2.  $\Lambda_\pi = 650$  MeV/c.

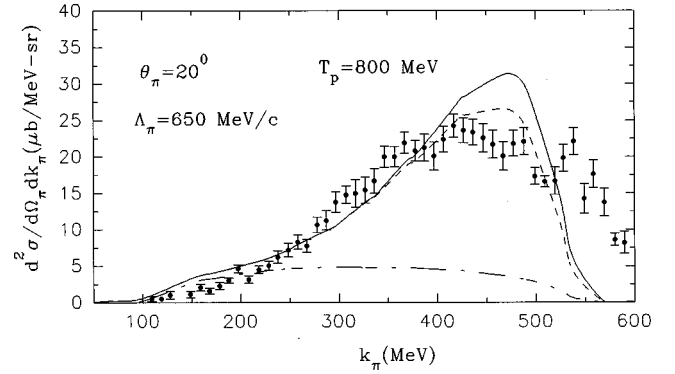


FIG. 4. The outgoing pion momentum spectra for the  ${}^2\text{H}(p, p' \pi^+)n$  reaction at  $T_p = 800$  MeV.  $\theta_\pi = 20^\circ$ . The experimental points are from Ref. [18]. The solid curve is calculated using both the  $\Delta^{++}$  and  $\Delta^+$  diagrams added coherently. The short-dashed and dot-dashed curves show separately the contribution due to  $\Delta^{++}$  and  $\Delta^+$ , respectively.  $\Lambda_\pi = 650$  MeV/c.

$$\mathbf{q} = \mathbf{k}_p - \mathbf{k}_\Delta [= (\mathbf{k}_N + \mathbf{k}_\pi)] - \frac{\omega \mathbf{k}_\Delta}{E_\Delta}, \quad (12)$$

where  $\omega$  is the energy transfer in exciting the  $\Delta$ . At the  $\pi NN$  vertex we replace

$$\mathbf{q}^2 \rightarrow -t, \quad (13)$$

where  $t$  is the four momentum squared.

### III. RESULTS AND DISCUSSION

Using the above formalism we calculate the exclusive proton momentum spectra, the outgoing pion momentum spectra, and the integrated total  ${}^2\text{H}(p, p' \pi^+)n$  cross section.

As the detailed measurements for the  ${}^2\text{H}(p, p' \pi^+)n$  process exist at 800 MeV beam energy, we first calculate the differential cross sections at this energy. In Fig. 2, we plot the calculated as well as the measured [6] exclusive proton momentum spectra for the proton and the pion angles of  $14.5^\circ$  and  $-21^\circ$ , respectively. These angles correspond to the  $\Delta$  going at  $0^\circ$ . The figure has four calculated curves. The short-dashed and dot-dashed curves correspond to  $\Delta^{++}$  and  $\Delta^+$  contributions (including both the “direct” as well as “exchange” diagrams), respectively. The solid curve is the coherent sum of these two contributions. We find that this curve agrees well with the measured cross sections. We also note that the main contribution to the solid curve comes from the  $\Delta^{++}$  diagram. The  $\Delta^+$  contributes only to the extent of 5–10%.

To show the contribution of the “exchange” diagram, in Fig. 2 we also show (by the long-dashed curve) the cross section for the  $\Delta^{++}$  diagram using only the “direct” term. Comparing this with the short-dashed curve, which includes both the direct and exchange diagrams, we find that the contribution of the exchange term is around 15–20%.

In Fig. 3, we show the proton spectrum for another set of proton and pion angles. This pair of angles also corresponds to the delta going at  $0^\circ$ . The outgoing proton and pion angles are  $14.5^\circ$  and  $-42^\circ$ , respectively. All the curves have the same meaning as those in Fig. 2. Here too the calculated proton spectrum is in good accord with the measured spec-

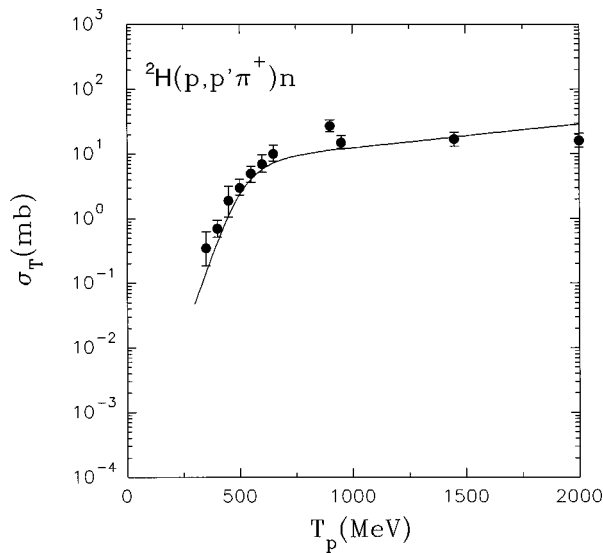


FIG. 5. Total cross section for the  ${}^2\text{H}(p,p'\pi^+)n$  reaction. The calculated curve includes both the direct and exchange  $\Delta^{++}$  excitation diagrams.  $\Lambda_\pi=650$  MeV/c. The experimental points are from Ref. [19].

trum. Other observations also remain same as in Fig. 2.

In Fig. 4 we show the double differential cross section as a function of the outgoing pion momentum. The proton angles are integrated. Experimentally such measurements exist for 800 MeV beam energy and the pion detected at  $20^\circ$  [18]. In this figure we have three curves along with the experimental data. The dash and dash-dot curves correspond

separately to the  $\Delta^{++}$  and  $\Delta^+$  diagrams, respectively. The solid curve is calculated including both the diagrams. All the curves include the direct as well as exchange diagrams. Excluding the peak in the measured cross sections around 550 MeV, the solid curve is in overall accord with the measured cross sections. Relative contributions of the  $\Delta^+$  and  $\Delta^{++}$  to the cross sections are at the same level as in the earlier curves. The peak around 550 MeV, as kinematic considerations suggest, may arise from the resonance structure between neutron and proton in the final state.

Finally in Fig. 5 we present the calculated total integrated cross section as a function of the beam energy from threshold to 2 GeV. Since, as seen from the results in Figs. 2–4, the contribution of the  $\Delta^+$  is only at the level of 10%, we give the calculated results for the  $\Delta^{++}$  only. The calculated results include both the direct and the exchange contributions. We find an excellent agreement between the calculated and measured cross sections [19].

#### IV. CONCLUSIONS

In conclusion, the findings of this paper can be summarized as follows. (1) Experimentally measured exclusive proton momentum spectra, the pion momentum spectrum, and the total integrated cross sections over a large energy range can be reproduced well with one-pion exchange potential for the  $\Delta$  excitation in the intermediate state. (2) The contribution of the  $\Delta^{++}$  dominates.  $\Delta^+$  contributes only to the extent of 5–10 %. (3) The effect of the exchange process is to bring down the cross section. Its contribution, however, is only at the level 10–20 %.

[1] V. Dmitriev, O. Sushkov, and C. Gaarde, Nucl. Phys. **A459**, 503 (1986).  
 [2] B. K. Jain and A. B. Santra, Nucl. Phys. **A519**, 697 (1990).  
 [3] B. K. Jain and A. B. Santra, Int. J. Mod. Phys. E **1**, 201 (1992).  
 [4] F. Shimuzu *et al.*, Nucl. Phys. **A386**, 571 (1982); **A389**, 445 (1982).  
 [5] D. V. Bugg *et al.*, Phys. Rev. **133**, B1017 (1964); S. Coletti *et al.*, Nuovo Cimento **49**, 479 (1967); A. M. Eisner *et al.*, Phys. Rev. **138**, B670 (1965); G. Alexander *et al.*, Phys. Rev. **154**, 1284 (1967); T. C. Bacon *et al.*, *ibid.* **162**, 1320 (1967).  
 [6] A. D. Hancock *et al.*, Phys. Rev. C **27**, 2742 (1983).  
 [7] B. K. Jain and Bijoy Kundu, Phys. Rev. C **53**, 1917 (1996); Bijoy Kundu and B. K. Jain, Phys. Lett. B **422**, 19 (1998).  
 [8] A. Engel *et al.*, Nucl. Phys. **A603**, 387 (1996).  
 [9] A. B. Wicklund *et al.*, Phys. Rev. D **34**, 19 (1986); **35**, 2670 (1987).  
 [10] B. K. Jain and A. B. Santra, Phys. Lett. B **244**, 5 (1990).  
 [11] B. K. Jain and A. B. Santra, Phys. Rev. C **46**, 1183 (1992).  
 [12] Q. Haider and L. C. Liu, Phys. Lett. B **335**, 253 (1994).  
 [13] V. F. Dmitriev, Nucl. Phys. **A577**, 249c (1994).  
 [14] D. Prout *et al.*, Nucl. Phys. **A577**, 233c (1994).  
 [15] C. Ellegard *et al.*, Phys. Lett. B **231**, 365 (1989).  
 [16] T. Sams and V. F. Dmitriev, Phys. Rev. C **45**, R2555 (1992).  
 [17] D. V. Bugg, A. A. Carter, and J. R. Carter, Phys. Lett. **44B**, 278 (1973); O. Dumbrajs *et al.*, Nucl. Phys. **B216**, 277 (1983); E. Oset, H. Toki, and W. Weise, Phys. Rep. **83**, 281 (1982); V. Flaminio, W. G. Moorhead, D. R. O. Morrison, and N. Rivoire, CERN Report No. CERN-HERA 83-01, 1983.  
 [18] P. R. Bevington, *Nucleon-Nucleon Interactions*, Vancouver (AIP, New York, 1977), p. 305.  
 [19] W. O. Lock and D. F. Measday (unpublished).